2021

Experimental Comparison of HCFO and HFO R1224yd(Z), R1233zd(E), R1336mzz(Z), and HFC R245fa in a High Temperature Heat Pump up to 150 °C Supply Temperature

Cordin Arpagaus
Eastern Switzerland University of Applied Sciences, Institute for Energy Systems, Werdenbergstrasse 4, 9471 Buchs, Switzerland, cordin.arpagaus@ost.ch

Stefan Bertsch

Experimental Comparison of HCFO and HFO R1224yd(Z), R1233zd(E), R1336mzz(Z), and HFC R245fa in a High-Temperature Heat Pump up to 150 °C Supply Temperature

Cordin ARPAGAUS* and Stefan S. BERTSCH

[1]Eastern Switzerland University of Applied Sciences of Technology, Institute for Energy Systems (IES), Werdenbergstrasse 4, 9471 Buchs, Switzerland

* Corresponding Author: cordin.arpagaus@ost.ch, +41 58 257 34 94

ABSTRACT

The use of industrial high-temperature heat pumps (HTHP) is particularly interesting for heat recovery applications and various industrial processes such as steam generation, drying, sterilization, paper production, or food preparation. The application of new synthetic hydrofluoroolefin (HFO) and hydrochlorofluoroolefin (HCFO) refrigerants with low environmental impact is becoming increasingly important in future HTHP.
At our university in Switzerland, a laboratory-scale HTHP has been developed as part of the SCCER-EIP project (Swiss Competence Center for Energy Research – Efficiency of Industrial Processes). The developed heat pump is single-stage, operates with a variable speed piston compressor, and contains a continuously adjustable internal heat exchanger (IHX) for superheating control. A viscous POE oil (173 mm^2/s at 40 °C) is used to achieve sufficient lubrication at high temperatures with the refrigerants.
This paper presents the experimental performance of the HCFO and HFO refrigerants R1224yd(Z), R1233zd(E), and R1336mzz(Z) as drop-in replacements for the fluorinated hydrocarbon (HFC) R245fa in the same laboratory HTHP with 10 kW heating capacity. Starting from a reference point at W60/W110 (50 K temperature lift), a parameter study was performed to investigate the operating maps (i.e. heating capacity and COP) of the heat pump in the range from 30 to 80 °C heat source and 70 to 150 °C supply temperature. Besides, an overview of the thermophysical, environmental, and safety aspects of the refrigerants is given.
At W60/W110 COPs of 3.2, 3.1, 3.0, and 3.1 for R1224yd(Z), R1233zd(E), R1336mzz(Z) and R245fa were measured. Up to about 110 °C, R1224yd(Z), R1233zd(E), and R245fa presented a slightly higher COP than R1336mzz(Z) due to higher heating capacities and lower relative heat losses at the same temperature conditions. Due to higher critical temperatures, R1336mzz(Z) was more efficient at 150 °C heat supply temperature. Otherwise, the differences in COP were within the measurement uncertainty of maximum ± 0.22 COP.
The integration of the IHX in the heat pump cycle significantly increased the COP and the heating capacity over the entire operating map compared to a basic cycle. A further COP increase was achieved by a higher temperature glide on the heat supply side from 5 to 30 K (increased subcooling), which is promising in processes with low return temperatures. The drop-in tests also showed that the heating capacity of R1224yd(Z) was on average 9% higher than that of R1233zd(E), which in practice requires slightly smaller compressors to achieve a comparable heating capacity. Overall, the very low GWP, the non-flammability, and the negligible environmental impact (i.e. low trifluoroacetic acid (TFA) formation during atmospheric degradation) of the investigated HCFO and HFO refrigerants indicate a high potential for future use in HTHP applications and retrofit systems.

Keywords: high-temperature heat pump, industrial heat pump, HCFO/HFO refrigerants, R1224yd(Z), R1233zd(E), R1336mzz(Z)

1. INTRODUCTION

1.1 Motivation

The use of electrically driven high-temperature heat pumps (HTHP) for industrial applications is expected to play a key role in achieving the political goals of climate neutrality by 2050. The replacement of fossil fuel-fired boilers with such kind of HTHP will help to decarbonize and electrify the industrial sector. The switch from fossil fuels to renewable energy sources will significantly reduce the CO_2 footprint. The use of industrial HTHP is particularly interesting for heat recovery applications and various industrial processes, such as process heat for food preparation, or low-pressure steam generation for sterilization and drying processes.

At least 26 industrial HTHP products have been identified on the market that are capable of delivering heat at 90 to 160 °C (Arpagaus 2018, Arpagaus al. 2017, 2018a, 2018b). On an international level, various experimental R&D projects are driving HTHP technology from the laboratory scale towards the industry. The main research objectives are (1) extending the limits of the heat source and heat sink temperatures to higher levels, (2) improvement of COP by multi-stage cycles and oil-free compressors, (3) development of temperature-resistant components, such as compressors and valves, and (4) developing and testing of environmentally friendly refrigerants (e.g. natural and synthetic) with low global warming potential (GWP).
The choice of suitable refrigerant is the subject of much debate. Most of the commercialized HTHP use the partially fluorinated hydrocarbon (HFC) R245fa as a refrigerant. However, R134a, R245fa, and R365mfc have a greenhouse effect (GWP of 1'300, 858, and 804 (Myhre *et al.*, 2013) and are experiencing a phase-down in production and consumption in most industrialized countries. In Europe, the F-gas regulation gradually reduces the market availability of greenhouse refrigerants. Consequently, only refrigerants with a GWP < 150 may be used in new commercial heat pumps starting from 2022. In Switzerland, the legal basis for refrigerants is regulated in the Chemicals Risk Reduction Ordinance (ChemRRV) (BAFU, 2019) and industrial heat pumps with heat source capacity > 600 kW are affected by the HFC ban. Besides, natural refrigerants, such as water (R718), CO_2 (R744), ammonia (R717), butane (R600), propane (R290), and pentane (R601), the application of the 4th generation of new synthetic hydrofluoroolefin (HFO) and hydrochlorofluoroolefin (HCFO) refrigerants is becoming increasingly important as drop-in replacements for HFC. Even though HCFO contain a chlorine atom in their structure and do not comply with the legal requirements of the Montreal Protocol (Ozone Depletion Potential, ODP of zero) there are national regulations, like the ChemRRV that allow the use of HCFO refrigerants with an ODP < 0.0005.

1.2 Objectives

A laboratory-scale HTHP has been developed as part of the SCCER-EIP project (Innosuisse, 2019). The developed laboratory HTHP is a single-stage vapor compression heat pump. The basic design of the HTHP (Arpagaus *et al.*, 2018, 2019) and various experimental results with R1233zd(E), R1336mzz(Z), and R1224yd(Z) have already been published in previous papers (Arpagaus *et al.*, 2019, 2018; Arpagaus & Bertsch, 2019).
This paper continues these studies and examines the performance of R1336mzz(Z) (Opteon^{TM} MZ, Chemours), R1233zd(E) (Forane®SCH 1233zd(E), ARKEMA), and R1224yd(Z) (AMOLEA^{TM}1224yd(Z), AGC Chemicals) experimentally in the same laboratory HTHP as drop-in replacements for R245fa (Genetron®245fa, Honeywell). Parameter studies are carried out with and without IHX to investigate the COP and heating capacity as a function of the temperature lift between 30 to 80 °C heat source and 80 to 150 °C heat sink temperatures. The performance data of the HCFO and HFO refrigerants are compared to R245fa as a baseline and available literature data.

2. REFRIGERANTS AND LITERATURE DATA OF EXPERIMENTAL STUDIES

Table 1 lists the most important thermodynamic, environmental, and safety properties of the investigated HFO and HCFO refrigerants R1336mzz(Z), R1233zd(E), R1224yd(Z) in comparison to HFC R245fa. Table 2 shows an overview of experimental studies performed by several researchers using HTHP prototypes using those refrigerants. In the course of this paper, the results obtained in this study will be compared to these literature data.

Table 1: Properties of the tested refrigerants R1224yd(Z), R1233zd(E), R1336mzz(Z), and R245fa.

Refrigerant	R1224yd(Z)	R1233zd(E)	R1336mzz(Z)	R245fa
Molecular structure	Z-CF_3-CF=CHCl	E-CF_3-CH=CHCl	Z-CF_3-CH=CHCF_3	CHF_2-CH_2-CF_3
Molecular weight (kg/kmol)	148,62	130,5	164,06	134,05
Normal boiling point (°C)	14,6	18,0	33,4	14,9
Critical temperature (°C)	155,5	165,6	171,3	154,0
Critical pressure (bar)	33,4	35,7	29,0	36,5
GWP_{100} (-)	0,88	1, <5	2	858
ODP (CFC-11 = 1) (-)	0,00023	0,00034, ,00030	0	0
Atmospheric lifetime (days)	20	~14, 26, 36, 40,4	22	7.7 years
Safety class (ASHRAE 34)	A1	A1	A1	B1
Degradation products	$CF_3C(O)OH$, CO_2, HF, HCl	CO_2, HF, HCl	CO_2, HF	CO_2, HF
TFA yield from atmospheric degradation (mol %)	97	~ 2	< 20	< 10

Table 2: Published experimental research studies testing HFO and HCFO refrigerants in HTHP systems.

Refrigerant	Heating capacity (kW)	Heat source/sink temperatures (°C)	Compressor type	Cycle type	Reference
R1224yd(Z) R245fa	320	50 to 70 / 95 to 115 60 to 75 / 85 to 95	Twin-screw HEM HR115	1-stage (IHX) and economizer	(Kaida *et al.*, 2019; Kobelco, 2019)
R1336mzz(Z)	12	30 to 110 / 75 to 160	Piston	1-stage (IHX)	(Helminger *et al.*, 2016)
R1336mzz(Z), R245fa	13 to 33	60 to 95 / 100 to 150	Piston (HeatBooster)	1-stage (IHX)	(Nilsson *et al.*, 2017)
R1336mzz(Z), R1336mzz(E), R245fa	75 to 200	80 to 130 / 110 to 140	4 pistons in parallel (HeatBooster S4)	1-stage (IHX)	(Hamacher, 2019)
R1233zd(E), R1336mzz(Z), R1224yd(Z)	3 to 10	30 to 80 / 80 to 150	Piston	1-stage (IHX) (adjustable)	(Arpagaus *et al.*, 2019; 2018; Arpagaus & Bertsch, 2019)
R245fa	11 to 18	60 to 80 / 90 to 140	Scroll	1-stage (IHX)	(Mateu-Royo *et al.*, 2019)

R1224yd(Z) is an HCFO refrigerant developed for use in centrifugal chillers, power generation in Organic Rankine Cycles (ORC) applications (Eyerer *et al.*, 2019), and HTHP for waste heat recovery (Fukushima, 2018). AGC Chemicals (Asahi Glass) markets R1224yd(Z) as Amolea®1224yd (AGC Chemicals, 2017; AGC Inc., 2018). The physical properties are close to R245fa. Its critical temperature is 155.5 °C and the saturated vapor pressure slightly lower (about 13% smaller at 120 °C) (Kaida *et al.*, 2019). Although R1224yd(Z) contains a chlorine atom that may participate in the catalytic destruction of the ozone layer, the atmospheric lifetime is sufficiently short with 20 days. With an ODP of almost zero (0.00023) and a GWP of 0.88 the environmental impact is estimated to be low (Tokuhashi *et al.*, 2018). Besides, it is classified as A1 (non-flammable and low-toxicity). The atmospheric oxidation of HCFO and HFO leads to final degradation products such as hydrofluoric acid (HF), hydrochloric acid (HCl), CO_2, and $CF_3C(O)OH$ (trifluoroacetic acid, TFA) (Wallington *et al.*, 2015). For R1224yd(Z) the molar yield of TFA formation by atmospheric degradation is about 97% (Guo *et al.*, 2019). This is attributed to the CF_3-CF= group.

Kaida *et al.* (2019) presented the first experimental results of R1224yd(Z) in a commercial HEM-HR115 heat pump (with economizer and IHX) developed by Kobelco and the Japanese electric utilities. Drop-in tests at W50/W95 revealed a 3% higher heating capacity and 12% higher COP compared to R245fa. The performance increase was attributed to a higher refrigerant mass flow rate, a lower viscosity, and a lower required pressure ratio (higher compressor efficiency). The chemical stability and compatibility with PAG (polyalkylene glycol) oil, O-rings, and motor insulation material were comparable to that of R245fa. Overall, R1224yd(Z) was suggested as a suitable R245fa alternative for HTHP. In September 2019, Kobelco (2019) announced the release of a 320 kW HTHP series HEM HR GN/GL with R1224yd(Z), which was jointly developed with Kimura Chemical Industries Co, Ltd. The HTHP system is capable of recovering 60 to 75 °C waste heat from condensers of distillation and concentration systems or an ammonia recovery unit to provide hot water at 95 °C with a COP of 7.5 (heat source: 73/68 °C in/out, heat sink: 90/95 °C in/out, 22 K temperature lift). The product is scheduled for market launch in 2020.

R1233zd(E) is available under the brand names Solstice®zd from Honeywell (2013) or as Forane®HTS 1233zd from ARKEMA (Rached *et al.*, 2018). Today, R1233zd(E) is mainly used as a blowing agent for duroplastic foams and aerosols. In air conditioning, it is used for large chillers with radial compressors (Kujak *et al.*, 2018). It is recommended for applications in HTHP and ORC. It has a critical temperature of 165.6 °C, a critical pressure of 35.7 bar, and is non-flammable (safety class A1). The atmospheric lifetime is sufficiently short, depending on the study, about 14 days (Andersen *et al.*, 2015), 26 days (Myhre *et al.*, 2013), 36 days (Sulbaek Andersen *et al.*, 2018), or 40.4 days (Patten & Wuebbles, 2010), so that the gas does not reach the stratosphere after the leakage and thus does not participate in ozone depletion. Depending on the study, an ODP of 0.00034 (Patten & Wuebbles, 2010) or 0.00030 (Sulbaek Andersen *et al.*, 2018) is reported. Its GWP is 1 (Myhre *et al.*, 2013) or < 5 (Sulbaek Andersen *et al.*, 2018). Due to a slightly different molecular structure than R1224yd(Z), the formation of TFA by atmospheric oxidation is almost negligible at ~ 2% (Sulbaek Andersen *et al.*, 2018). At high operating temperatures, a small amount of R1233zd(E) can isomerize to R1233zd(Z). Stabilizers can significantly reduce Z-isomer formation. As confirmed by Rached *et al.* (2018), stabilized R1233ze(E) showed a very low degree of isomerization (< 0.5%) at 220 °C and 14 days of aging.

R1336mzz(Z) has a high critical temperature of 171.3 °C at a feasible pressure of 29.0 bar. Chemours commercialized R1336mzz(Z) under the brand Opteon™MZ for waste heat recovery in HTHP and ORC applications. The fluid is stable to more than 225 °C and can enable condensation temperatures above 160 °C. It is safety class A1, has a GWP of 2, an ODP of 0, and a relatively short atmospheric lifetime of 22 days (Myhre *et al.*, 2013). In terms of TFA degradation in the atmosphere, R1336mmz(Z) is expected to decompose to < 20 % TFA due to the molecular structure

containing two CF_3-CH= groups (Henne *et al.*, 2012). Polyolester oil (POE) is recommended as a lubricant, as it is fully miscible over wide ranges of temperatures and compositions (Kontomaris, 2014a, 2014b). The commercial HeatBooster S4 from Viking Heat Engines (2018) represents the industrial benchmark with heat sink outlet temperatures of up to 165 °C using R1336mzz(Z) and a nominal heating capacity of 200 kW. The HeatBooster S4 consists of 4 piston compressors connected in parallel with a combined evaporator and condenser. Nilsson *et al.* (2017) measured the performance of the main components of the HeatBooster system in an IHX cycle with 1 piston compressor and R1336mzz(Z) with a heating capacity of about 30 kW. Heat pump tests demonstrated a heating COP of 4.6 and 2.7 at 90 °C heat source and 130 °C and 150 °C heat sink, respectively. The commercial HeatBooster S4 with R1336mzz(Z) achieves a COP of 4.1 at 90°C/130°C and 100/140°C (heat source/sink), as recently presented by Hamacher (2019). In the laboratory scale, Helminger *et al.* (2016) applied R1336mzz(Z) (previously referred to as DR-2) and reported a highest heat sink outlet temperature of 156.3 °C (condensation at 160 °C) in a single-stage laboratory HTHP with IHX with a COP of 2.67 and a temperature lift of 47.4 K. In a previous study, Fleckl *et al.* (2015) reached 150 °C in a basic cycle with a COP of 2.4 and a temperature lift of 70 K.

R245fa is a non-ozone depleting fluid for use in centrifugal chillers (Honeywell, 2011). Today it is the main refrigerant in industrial HTHP because it offers a relatively high critical temperature of 154.0 °C at moderate pressures of 36.4 bar. However, R245fa will be phased out in the foreseeable future due to a high GWP of 858 (Myhre *et al.*, 2013) and atmospheric life of 7.7 years (WMO, 2011). Nevertheless, it is used as a reference fluid for drop-in replacement tests with refrigerants having lower GWP like HFO and HCFO (Hamacher, 2019; Helminger *et al.*, 2016; Kaida *et al.*, 2019; Nilsson *et al.*, 2017). Recently, Mateu-Royo *et al.* (2019) presented a single-stage HTHP system with a scroll compressor using R245fa for waste heat recovery. The prototype achieved a heat sink temperature of 140 °C with a COP of 2.23 at an 80 °C heat source. The highest reported COP was 3.41 obtained at 80 °C/110 °C.

Based on the above discussed literature review, it can be seen that the HTHP technology with HFO and HCFO refrigerants is at an early stage. Thus, the purpose of this paper is to present the first experimental results with R1233zd(E), R1336mzz(Z), R1224yd(Z), and R245fa in the same HTHP laboratory system in comparison.

3. EXPERIMENTAL SETUP AND TEST PROCEDURE

3.1 Experimental setup

Figure 1 illustrates the laboratory HTHP and its schematic diagram. The system design has been described in detail in earlier conference contributions (Arpagaus *et al.*, 2019, 2018; Arpagaus & Bertsch, 2019). The HTHP has a single-stage design and operates with a variable-speed semi-hermetic piston compressor (Bitzer, 2DES-3Y New Ecoline). An external frequency converter (Vacon 100) adjusts the compressor speed within the permissible limits (30 to 60 Hz corresponds to 870 to 1'750 rpm). An integrated temperature sensor prevents the motor windings from overheating with a switch-off temperature of approx. 110 °C. The fan for compressor cooling was not in operation during the experiments. A three-way valve (Siemens, M3FK15LX15) in the cycle allows adjustment of the refrigerant flow through the IHX from 0 to 100%, where a setting of 0% IHX corresponds to the operation of a basic cycle, while at 100% the IHX is completely flowed through.

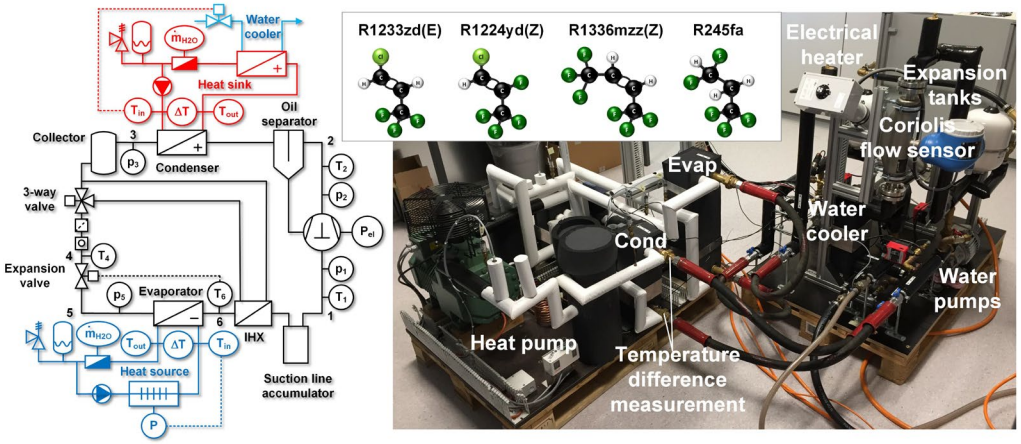

Figure 1: Laboratory HTHP for testing low GWP HFO and HCFO refrigerants up to 150 °C heat sink temperature (left: principle drawing, right: with the heat source and sink circuits connected to the HTHP).

The superheat is measured between the evaporator and the IHX (T_6) and is set to 5 K ($\Delta T_{SH} = T(p_5) - T_6$) for all tests unless otherwise specified. It is controlled by an electronic expansion valve (Siemens, MVL661.15-0.4) and PI control in LabVIEW™. The integration of the IHX increases the suction gas temperature (T_1), which ensures dry compression and simultaneously subcools the refrigerant after condensation. The heat exchangers are compact plate-type heat exchangers with low pressure drop. A suction gas accumulator (ESK Schultze, FA-22) prevents the direct penetration of liquid refrigerant into the compressor. A liquid receiver (5.6 L, Bitzer FS56) serves as a refrigerant collector after condensation and ensures liquid refrigerant before the expansion valve. The optimized refrigerant charges for R1336mzz(Z), R1233zd(E), R1224yd(Z), and R245fa were 4.1, 3.5, 3.6, and 3.5 kg, respectively. To determine the optimum refrigerant charge, the HTHP was operated at (Ref) conditions W60/W110, and the COP was checked as a function of the amount of refrigerant added in about 200 g steps. Besides, the sight glass in the liquid line was checked for clarity (no gas bubbles). An oil change was carried out between refrigerant changes and the HTHP cycle was evacuated overnight to minimize residual moisture in the system.

A polyol ester (POE) oil (Fuchs, Reniso Triton SE 170) with a viscosity of 173 mm²/s at 40 °C (17.6 mm²/s at 100 °C) was used to achieve sufficient lubrication at high operating temperatures and complete miscibility with the refrigerants. A coalescent oil separator (Temprite, Coalescent 922M) is installed on the high-pressure side, which traps the oil and returns it to the compressor via a cooling pipe. As a safety measure, a high-pressure/low-pressure pressostat protects the compressor and all other components. A filter dryer is integrated in the system to absorb residual moisture. Compared to the first experimental test results with R1233zd(E) (Solstice®zd, Honeywell, 2013) presented at Purdue Conferences in 2018 (Arpagaus *et al.*, 2018), the insulation of the oil separator, copper lines on the hot gas side, liquid receiver, and suction line accumulator was improved with temperature resistant Armaflex®HT insulation. An average COP improvement of 21 ± 7% was achieved based on 5 operating points with R1233zd(E) in the IHX cycle.

The temperatures are measured with calibrated thermocouples (Type K, class 1) with an accuracy of ± 0.1 K. Differential temperature measurements are used at the inlet and outlet of the heat sink and source. A Coriolis flowmeter (E+H, Promass F300) measures the water mass flow in the heat sink circuit with an accuracy of ± 0.05 %. A power transmitter (Infratek, ITL-101) measures the electrical power consumption of the compressor before the frequency converter with an accuracy of ± 0.2% of the measurement range. A CompactRIO® cRIO-9022 platform from National Instruments in combination with LabVIEW™2017myRio is used for data acquisition and controlling the experimental set-up. The electrical heater controls the heat source inlet temperature ($T_{Source,in}$) and a control valve (BELIMO, 2-way zone valve with rotary actuator) at the inlet of the water cooler controls the heat sink inlet temperature ($T_{Sink,in}$) into the condenser (both by PI controls in LabVIEW™).

3.2 Test procedure

Figure 2 shows some typical temperature profiles of test runs with the HTHP. Tests were carried out at 30 to 80 °C at heat source inlet temperature ($T_{Source,in}$) and 70 to 150 °C heat sink outlet temperature ($T_{Sink,out}$) providing external temperature lifts ($\Delta T_{lift} = T_{Sink,out} - T_{Source,in}$) of 30 to 70 K. The heat source simulates potentially available waste heat from an industrial process. The heat sink represents a potential steam generation or drying application.

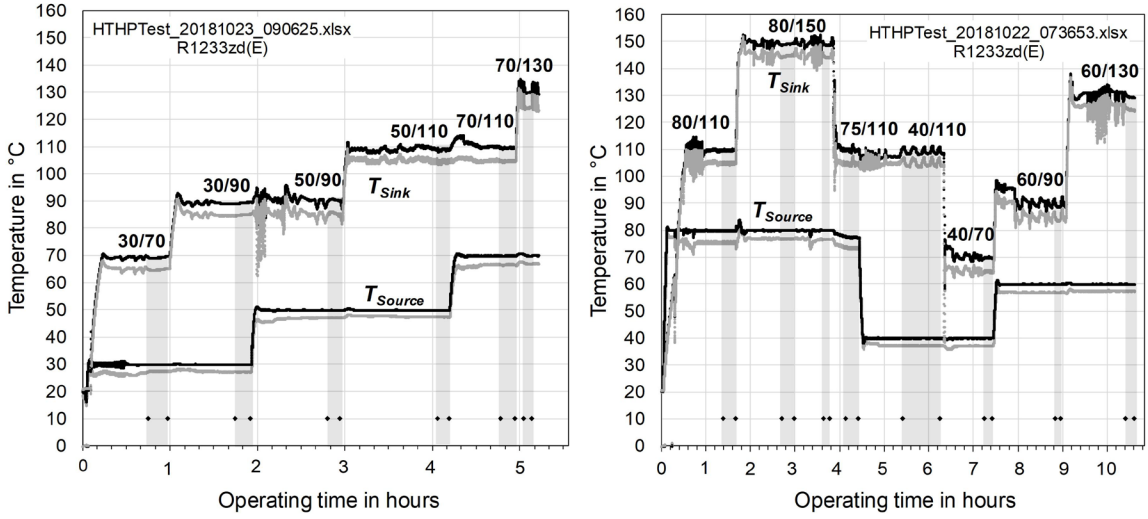

Figure 2: Temperature profiles of some test runs with stable conditions for the evaluation of the measuring points.

After heating the HTHP to the desired temperatures, the water flow rates in the two hydraulic loops are adjusted by the water pumps (Speck) to receive constant temperature differences (glides) of 3.0 ± 0.1 K at a heat source (ΔT_{Source}) and 5.0 ± 0.1 K at the heat sink (ΔT_{Sink}), which corresponds to the test standard DIN EN 14511 (unless otherwise specified). For each data point, mean values of at least 5 minutes were used for data analysis. The heating COP was determined from the measured heating capacity ($\dot{Q}_{Sink}$) and the electrical power consumption of the compressor (P_{el}) according to Eq. (1). The 2nd Law efficiency (η_{2nd}) was determined by Eq. (2). The temperature dependence of the specific heat capacity of water ($c_{p,H_2O}(T)$) was taken into account.

$$COP = \dot{Q}_{Sink}/P_{el} = \left(\dot{m}_{H_2O} \cdot c_{p,H_2O}(T) \cdot \Delta T_{Sink}\right)/P_{el} \quad (1)$$

$$\eta_{2nd} = COP_H/COP_{Carnot} \text{ with } COP_{Carnot} = T_{Sink,out}/\left(T_{Sink,out} - T_{Source,in}\right) \quad (2)$$

The error propagation according to the RSS method (Root Sum Squares) resulted in maximal uncertainties of $\Delta\dot{Q}_{Sink}$ ± 0.3 kW, ΔP_{Comp} ± 0.035 kW, and ΔCOP ± 0.22 over the entire operating map.

4. EXPERIMENTAL RESULTS AND DISCUSSION

4.1 Results with R1233zd(E)

Figure 3 (A) shows the COP of the HTHP with R1233zd(E) in basic and IHX cycle configuration as a function of the investigated heat sink temperature at different temperature lifts from 30 K to 70 K. As expected, the COP increases with smaller ΔT_{Lift} and higher $T_{Sink,out}$. At (Ref)-conditions (W60/W110), a COP of 3.2 was reached. Compared to the basic cycle, the integration of the IHX resulted in a COP increase of about 16%. The maximum tested heat sink temperature was 150 °C from a heat source at 80 °C with a COP of 1.5 (70 K lift).

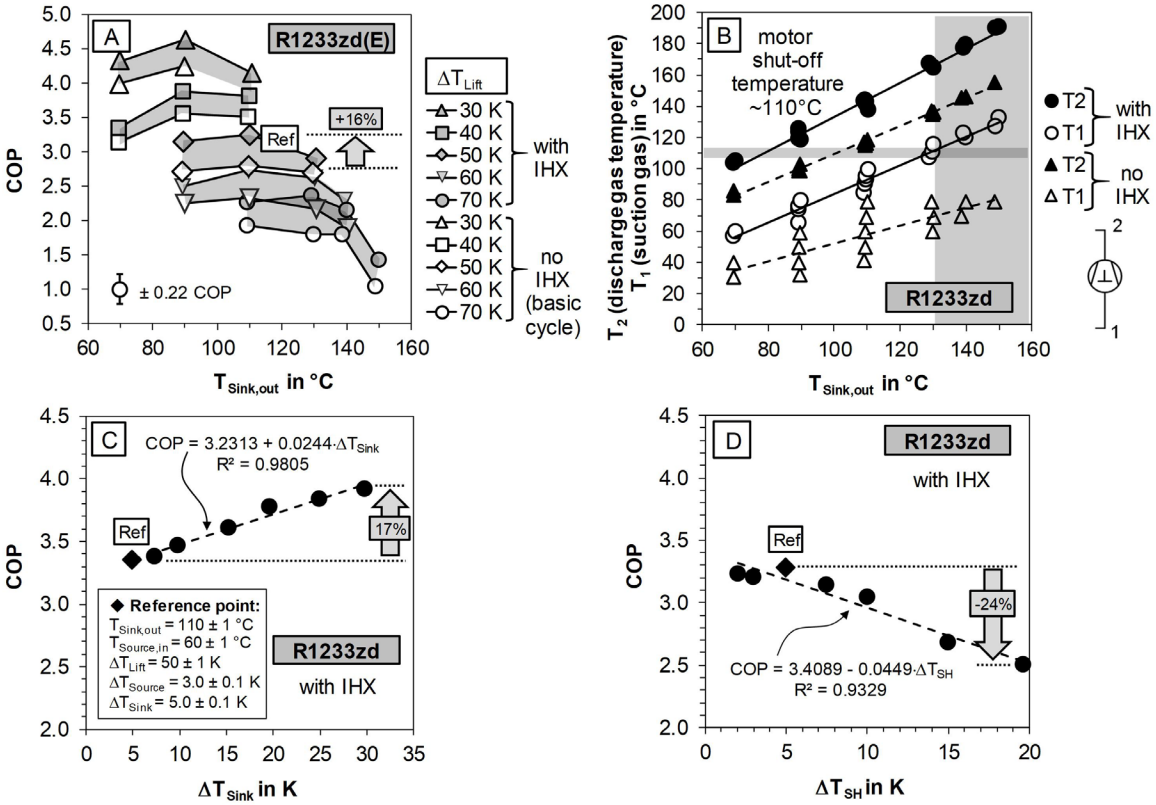

Figure 3: Experimental test results with R1233zd(E) in the laboratory HTHP.
(A) Influence of the IHX integration on the COP at different temperature lifts (with/no IHX),
(B) Discharge and suction gas temperature in function of the heat sink temperature (with/no IHX),
(C) Efficiency increase with higher temperature glide on the heat sink side (IHX cycle),
(D) Efficiency decrease with higher superheat after the evaporator (IHX cycle).

The decreasing COP curves at higher sink temperatures are a result of the smaller enthalpy of vaporization for condensation near the critical temperature and the increasing heat loss of the system due to natural convection and radiation. Depending on the temperature, heat losses of about 26 ± 6% are estimated from the energy balance of the heat pump ($\dot{Q}_{Loss} \approx \dot{Q}_{Source} + P_{Comp} - \dot{Q}_{Sink}$) leading to 2nd Law efficiencies (η_{2nd}) of 39 ± 3%. This means that there is still significant potential for optimization in insulation, especially at the compressor, and thus room for efficiency increase. In a large-scale application, the relative heat losses will be significantly lower due to the higher energy density of the heat pump and potential compressor cooling devices.

Figure 3 (B) illustrates the measured discharge (T_2) and suction gas (T_1) temperatures as a function of the $T_{Sink,out}$ for R1233zd(E). In the basic cycle, T_1 was clearly below the motor switch-off temperature of approx. 110 °C (grey line), whereas in the IHX cycle the temperature exceeded the motor limit temperature at approx. 130 °C and higher. However, short-term tests over several minutes at 150 °C were possible. On average, T_2 was approx. 34 K above $T_{Sink,out}$. Overall, the discharge temperatures were below 200 °C, which can be assumed as a conservative upper limit for the stability of the POE oil.

Figure 3 (C) shows the effect of a higher heat sink temperature glide (ΔT_{Sink}) on the COP varied from (Ref)-conditions as an example of a potential process heating application with low return temperatures (e.g. air heating for drying processes). With increasing ΔT_{Sink} from 5 K to 30 K (at constant $T_{Source,in}$) the heat transfer in the condenser improves, which led to a 12 % higher heating capacity (6.8 kW to 7.7 kW) and approx. 17 % higher COP.

Figure 3 (D) illustrates the influence of superheat ΔT_{SH} (state point between evaporator and IHX) on the COP, while keeping the other parameters constant at (Ref)-conditions. With higher superheat the evaporating temperature decreases and the required pressure ratio of the compressor increases, which reduces the efficiency. A superheat of 5 K was found to be a reasonable setting for the parameter study.

Overall, the measured performance data of Forane®SCH 1233zd are comparable to data with Honeywell's Solstice®zd R1233zd(E) already presented by Arpagaus *et al.* (2019). The same chemical substance gives similar results, which is not surprising. The relative deviations between both refrigerants were within ± 0.1 COP, therefore below measurement uncertainty.

4.2 Results with R1336mzz(Z)

Figure 4 (A) and (B) compares the measured performance maps of the refrigerant R1336mzz(Z) in the HTHP with the IHX cycle at similar temperature lifts with literature data from Helminger *et al.* (2016) (12 kW lab-scale), Nilsson *et al.* (2017) (30 kW HeatBooster, 1 piston), and Hamacher (2019) (150 kW HeatBooster, 4 pistons).

A 2nd Law efficiency of 34 ± 3% was obtained, which is in line with the laboratory setup of Helminger *et al.* (2016). Helminger *et al.* (2016) reported heat sink temperatures of up to 156.3°C and a COP of almost 2.7 with a temperature lift of about 45 K. Moreover, COPs of 5.5 were achieved at around 20 K lift. The HeatBooster technology achieves a higher η_{2nd} efficiency with 41 ± 3 % (Nilsson et al., 2017). Even at a 60 K temperature lift, a COP of 2.5 is achieved. This increase in performance is partially attributable to larger temperature glides tested on the heat sink of 10 K and 20 K, compared to 5 K in this study, which generally leads to an increase in efficiency (as shown in Figure 3 C for R1233zd(E)). In addition, with a larger heating capacity, the relative heat losses are smaller.

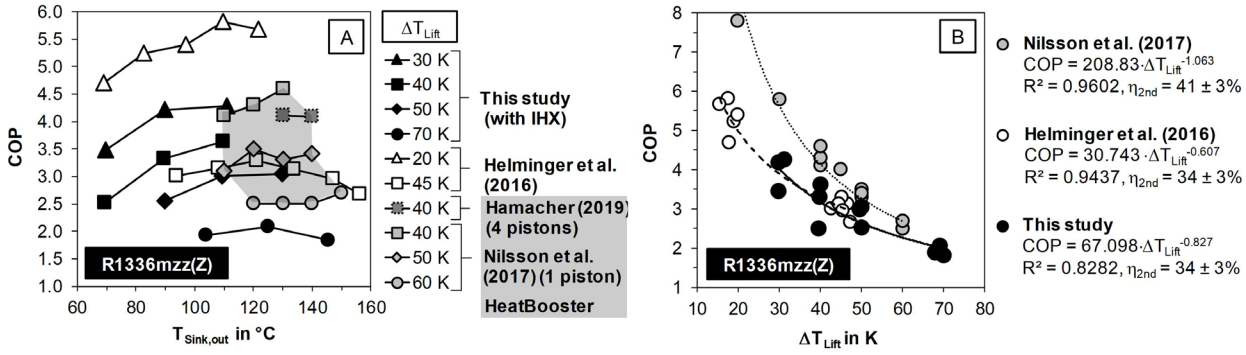

Figure 4: Comparison of the R1336mzz(Z) results with literature data of Helminger *et al.* (2016) (12 kW lab-scale), Nilsson *et al.* (2017) (30 kW HeatBooster, 1 piston), and Hamacher (2019) (150 kW HeatBooster, 4 pistons).

4.3 Results with R245fa

Figure 5 shows the COP data of R245fa. The COP advantages of using an IHX are visible in Figure 5 (A). For example, a COP improvement of up to 29% was achieved at W80/W130 by including the IHX. Figure 5 (B) compares the R245fa results with laboratory data from Mateu-Royo *et al.* (2019) using a scroll compressor and Nilsson *et al.* (2017) with the HeatBooster piston. As with R1336mzz(Z), the HeatBooster is more efficient (η_{2nd} up to 52%). On a labscale, the derived COPs of this study are higher than the values reported by Mateu-Royo *et al.* (2019), e.g. 32% higher at 60/90°C (4.43 vs. 3.35), 26% at 60/110°C (3.13 vs. 2.49), and 12% at 80/130°C (2.89 vs. 2.58). This is mainly attributed to a lower IHX effectiveness and the differences in the laboratory setups with a modified open scroll compressor. In the case of Mateu-Royo *et al.* (2019), the IHX effectiveness was a maximum of 0.38 compared to 0.66 ± 0.05 in this study, which suggests an IHX with a larger heat exchanger area and higher heat transfer rates.

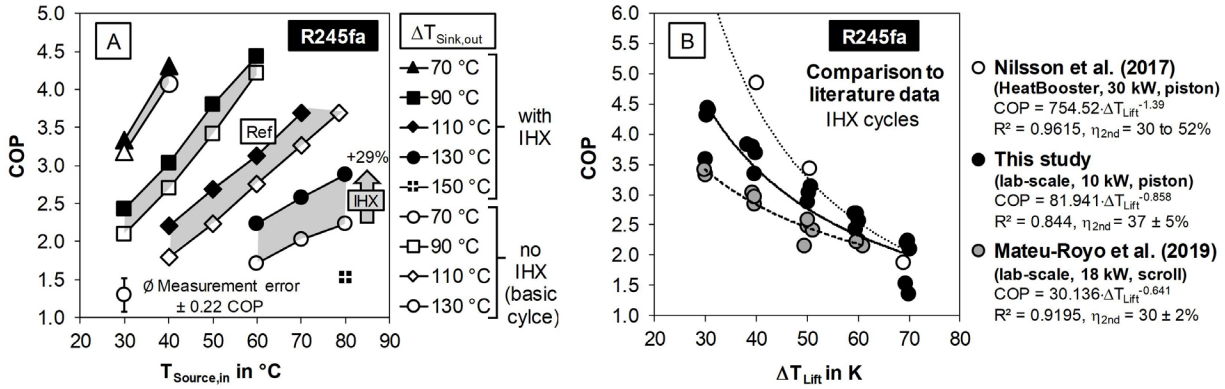

Figure 5: Test results with R245fa in the HTHP. (A) Influence of the IHX integration on the COP at different temperature conditions, (B) Comparison with data from Mateu-Royo *et al.* (2019) and Nilsson *et al.* (2017).

4.4 Comparison of all tested refrigerants

Figure 6 (A) to (D) compares the results of all tested refrigerants in the IHX cycle. The data of R245fa are colored red and used as a reference. Figure 6 (A) and (B) show the evident increase in efficiency with higher $T_{Source,in}$, lower $T_{Sink,out}$, and lower ΔT_{Lift}. The COP data are quite comparable. At (Ref)-conditions (W60/W110), COPs of 3.2, 3.1, 3.0, and 3.1 were achieved for R1224yd(Z), R1233zd(E), R1336mzz(Z), and R245fa, respectively.

Up to a $T_{Sink,out}$ of about 110 °C, R1224yd(Z), R1233zd(E), and R245fa delivered a slightly higher COP than R1336mzz(Z), which is attributed to the higher heating capacities (Figure 4, C) and the smaller relative heat losses at the same temperature conditions. The slightly decreasing COP curves at higher temperatures result from the narrower two-phase region for condensation near the critical point and the increasing heat losses of the system. Average heat losses of about 26 ± 6% were estimated from the energy balance, with the main origin at the compressor, as infrared camera analyses confirmed. At higher temperatures, the deviations in the COPs were within the measurement uncertainty of maximum ± 0.22 COP. The highest heat sink outlet temperature tested was 150 °C, whereby a COP of 1.8 was achieved with R1336mzz(Z) at 80 °C heat source. Due to the higher critical temperature of 171.3°C R1336mzz(Z), higher condensing temperatures can potentially be achieved. Further increases in efficiency could be achieved by better insulation of the heat pump components and pipes. A technical possibility to reduce heat losses is the installation of a tailor-made oil cooler, whose energy can be fed into the heat sink (e.g. hot water). Larger piston compressors could be optionally equipped with water-cooled cylinder heads. For practical applications with high temperature lifts, two-stage heat pump systems are more efficient (Arpagaus *et al.,* 2019).

Figure 6 (C) shows the heating capacity ($\dot{Q}_{Sink}$) as a function of $T_{Source,in}$ at constant ΔT_{Lift}. The heating capacity increased steadily with temperature. Overall, the heating capacity of R1336mzz(Z) was substantially lower than that of the other refrigerants. This is due to the lower volumetric heating capacity ($VHC = \rho_1(h_2 - h_3)$), which demands a compressor with a larger swept volume to achieve similar heating capacities. At (Ref)-conditions R245fa, R1233zd(E), R1224yd(Z), and R1336mzz(Z) provided a heating capacity of 7.9 kW, 7.5 kW (-5% relative to R245fa), 6.8 kW (-13%), and 4.3 kW (-45%), respectively. At W80/W130 the capacity limit of the laboratory system of approx. 10 kW was reached. With R1336mzz(Z) a maximum heating capacity of 7.8 kW could be achieved (W80/W111). The heating capacity of R1224yd(Z) was on average 9% higher than that of R1233zd(E). These findings are consistent with simulation studies by Arpagaus *et al.* (2019), where VHC values of 1'600 kJ/m^3 (-47% relative to R245fa),

2'412 kJ/m³ (-15%), 2'639 kJ/m³ (-7%), and 2'830 kJ/m³ were calculated for R1336mzz(Z), R1233zd(E), R1224yd(Z), and R245fa in a single-stage cycle with IHX at W60/W110. A compromise between COP and VHC needs to be found depending on the refrigerant.

Figure 6 (D) shows the COP data as a fit curve $COP = A \cdot \Delta T_{Lift}{}^{B}$ with a 2nd Law efficiency (η_{2nd}) of 39 ± 3% for R1233zd(E), 37 ± 5% for R1224yd(Z), 34 ± 3% for R1336mzz(Z), and 37 ± 5% for R245fa. The differences are mainly due to the higher or lower rated heat losses.

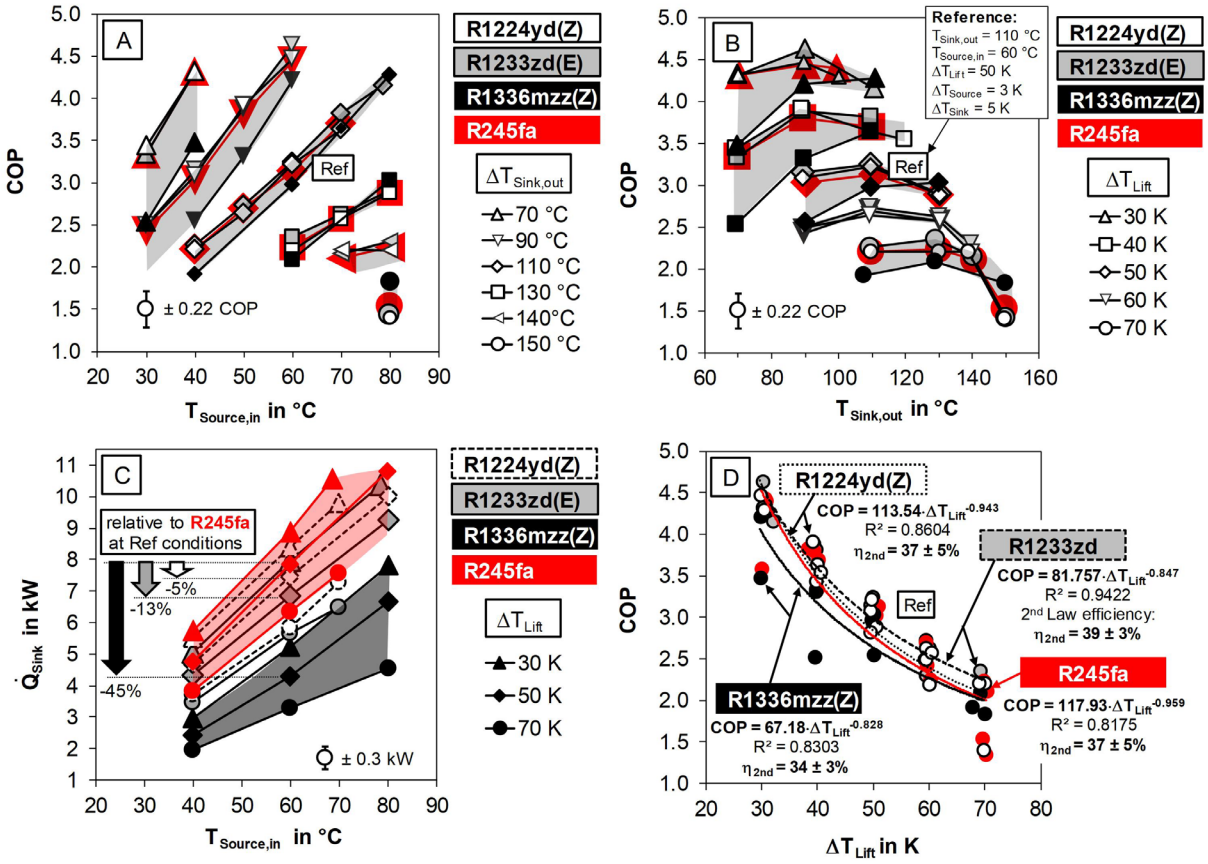

Figure 6: Comparison of the refrigerants R1224yd(Z), R1233zd(E), R1336mzz(Z), and R245fa. (A) COP vs. heat source inlet temperature ($T_{Source,in}$) at different heat sink outlet temperatures ($T_{Sink,out}$), (B) COP as a function of $T_{Sink,out}$ at different ΔT_{Lift}, (C) Heating capacity ($\dot{Q}_{Sink}$) vs. $T_{Source,in}$ at ΔT_{Lift} of 30, 50, and 70 K (relative difference to R245fa at Ref-conditions), (D) COP fit curves with 2nd Law efficiencies (η_{2nd}).

Finally, the acid number (neutralization number, mgKOH/g oil) of the POE oils was measured by manual colorimetric titration according to DIN 51558-1 as a measure of oil degradation. The POE oils were analyzed after about 100 operating hours in the HTHP after each refrigerant test campaign. Fresh oil was also measured for comparison. Visual inspections revealed a slightly yellowish color of the oils after the operation in the HTHP. Overall, hardly any oil degradation was detected. The acid number for fresh POE oil was 0.04, after the tests with R1233zd(E) 0.09, with R1336mzz(Z) 0.05, and with R1224yd(Z) 0.25, thus significantly below the 0.5 warning value assumed by the oil supplier for HTHP applications. The data confirm the principle suitability of POE oil for use with HFO and HCFO refrigerants. At best, even more viscous oils (e.g. PAG, or POE SE 220 with a viscosity of 19.0 mm²/s at 100 °C) and the addition of thermal stabilizers could to be tested. However, long-term tests were not the aim of this study. The measured suction gas temperatures (T_1) in the laboratory HTHP exceeded the motor limit temperature of approx. 110 °C at a heat sink outlet temperature of 130 °C and higher. However, short-term experiments over several minutes at 150 °C were still possible to run.

In any case, temperature-resistant compressors and thermally stable lubricating oils are crucial components for the further development and commercialization of HTHPs. An ideal solution would be the combination of a special motor that can withstand high temperatures and highly viscous and thermally stable oil that does not need to be cooled.

5. CONCLUSIONS

R1224yd(Z), R1233zd(E), R1336mzz(Z), and R245fa have been successfully tested in a laboratory HTHP with IHX cycle and up to 10 kW heating capacity. Compared to available literature data, this study offers for the first time a direct performance comparison of these refrigerants up to 150 °C supply temperature in the same HTHP system. The performance of the heat pump was demonstrated at 30 to 80 °C heat source and 70 to 150 °C heat sink temperatures (30 to 70 K temperature lifts) for possible applications of waste heat recovery, steam generation, or drying processes. The COP data ranged between 1.4 and 4.6 depending on the temperature conditions and were comparable across the entire operating maps. The differences in COP were within the measurement uncertainty of maximum ± 0.21 COP. Up to heat sink temperatures of about 110 °C, R1336mzz(Z) had a slightly lower COP due to the lower heating capacity and higher relative heat losses at the same temperature conditions. Relative to R245fa, the heating capacity of R1233zd(E), R1224yd(Z), and R1336mzz(Z) was 5%, 13%, and 45% lower at the operating point W60/W110, which is in agreement with previous simulation studies. The heating capacity of R1224yd(Z) was on average 9% higher than that of R1233zd(E) due to the lower boiling temperature. At W60/W110, COPs of 3.2, 3.1, 3.0, and 3.1 were measured for R1224yd(Z), R1233zd(E), R1336mzz(Z), and R245fa, respectively. A further COP increase of approx. 17 % was achieved by a higher temperature glide on the heat sink from 5 K to 30 K, improving the heat transfer in the condenser and increasing subcooling, which is promising for applications with low return temperature. Compared to the base cycle, the integration of the IHX resulted in a significant COP increase in the range of about 16% (R1233zd(E), W50/W110) to 29% (R245fa, W80/W130). This is attributed to the higher suction gas density at the compressor inlet due to the additional superheating with the IHX, which leads to increased heating capacity and efficiency. Investigations of the acid number of the POE oils after about 100 operating hours in the HTHP revealed a low oil degradation. The acid numbers were in the range of 0.05 to 0.25, and thus well below the warning value of 0.5 assumed by the oil supplier for HTHP applications. The developed HTHP enables the testing of other relevant HFO refrigerants, such as R1336mzz(E) and R514A, or other oils (e.g. POE, PAG) in the future. Further efficiency improvements could be achieved by reducing the thermal losses with better insulation of the heat pump components (especially the compressor). The installation of an oil cooler and water-cooled cylinder heads are further technical options to improve HTHP efficiency. In a further step, a detailed model of the HTHP would be desirable for scale-up, costs, and efficiency optimization.

NOMENCLATURE

COP	coefficient of performance (–)	T	temperature (°C)
$c_{p,H_2O}(T)$	specific heat capacity (kJ/kg-K)	ΔT	temperature difference (glide) (K)
GWP	global warming potential, 100 years	TFA	trifluoroacetic acid
h	enthalpy (kJ/kg)	VHC	volumetric heating capacity (kJ/m^3)
HCFO	hydrochlorofluoroolefin	W	water
HFC	hydrofluorocarbon	η_{2nd}	2nd Law efficiency (Carnot efficiency) (%)
HFO	hydrofluoroolefin	A, B	constants (–)
HTHP	high temperature heat pump		
IHX	internal heat exchanger	**Subscripts**	
$\dot{m}_{H_2O}$	water mass flow rate (kg/s)	Comp	compressor
ODP	ozone depletion potential	Cond	condensation, condenser
p	pressure (bar)	Crit	critical temperature
P_{el}	electrical power (kW)	Evap	evaporation, evaporator
PAG	polyalkylene glycol	in, out	inlet, outlet
POE	polyol ester	Lift	temperature lift
$\dot{Q}$	capacity (kW)	Loss	heat losses
Ref	reference point (W60/W110)	Sink	heat sink
ρ	density (kg/m^3)	Source	heat source
SG	safety group classification	1 … 6	state points numbering

REFERENCES

AGC Chemicals. (2017). *AMOLEA® 1224yd, Technical Information, ASAHI Glass Co., Ltd.* (pp. 1–18).

AGC Inc. (2018). New Generation Low GWP Refrigerant AMOLEA 1224yd. *Chillventa, Nuremberg, Oct. 16-18*.

Andersen, L. L., Østerstrøm, F. F., Sulbaek Andersen, M. P., Nielsen, O. J., & Wallington, T. J. (2015). Atmospheric chemistry of cis-CF3CHCHCl (HCFO-1233zd(Z)): Kinetics of the gas-phase reactions with Cl atoms, OH radicals, and O3. *Chemical Physics Letters*, *639*, 289–293. https://doi.org/10.1016/j.cplett.2015.09.008

Arpagaus, C. (2018). *Hochtemperatur-Wärmepumpen: Marktübersicht, Stand der Technik und Anwendungspotenziale, 138 Seiten, ISBN 978-3-8007-4550-0 (Print), ISBN 978-3-8007-4551-7 (E-Book)*. VDE Verlag GmbH.

Arpagaus, C., & Bertsch, S. S. (2019). Experimental results of HFO / HCFO refrigerants in a laboratory scale HTHP with up to 150 °C supply temperature. *2nd Conference on High Temperature Heat Pumps, September 9, 2019, Copenhagen*, 1–9. https://doi.org/https://orbit.dtu.dk/en/publications/book-of-presentations-of-the-2nd-symposium-on-high-temperature-he

Arpagaus, C., Bless, F., Schiffmann, J., & Bertsch, S. S. (2017). Review on High Temperature Heat Pumps – Market Overview and Research Status. *International Workshop on High Temperature Heat Pumps, September 9, 2017, Copenhagen, Denmark*, 1–25. https://backend.orbit.dtu.dk/ws/portalfiles/portal/138357883/Collection_of_Presentations_International_Workshop_on_High_Temperature_Heat_Pumps.pdf

Arpagaus, C., Bless, F., Uhlmann, M., Büchel, E., Frei, S., Schiffmann, J., & Bertsch, S. S. (2019). High temperature heat pump using HFO and HCFO refrigerants - System design, simulation, and first experimental results. *ICR 2019, The 25th IIR International Congress of Refrigeration, August 24-30, Montréal, Québec, Canada*, 1–9. https://doi.org/10.18462/iir.icr.2019.242

Arpagaus, C., Bless, F., Uhlmann, M., Büchel, E., Frei, S., Schiffmann, J., & Bertsch, S. S. (2018). High temperature heat pump using HFO and HCFO refrigerants - System design, simulation, and first experimental results. *17th International Refrigeration and Air Conditioning Conference at Purdue, July 9-12, 2018*, 1–10. https://doi.org/https://docs.lib.purdue.edu/iracc/1875

Arpagaus, C., Bless, F., Uhlmann, M., Schiffmann, J., & Bertsch, S. S. (2018a). High temperature heat pumps: Market overview, state of the art, research status, refrigerants, and application potentials. *Energy*, *152*, 985–1010. https://doi.org/10.1016/j.energy.2018.03.166

Arpagaus, C., Bless, F., Uhlmann, M., Schiffmann, J., & Bertsch, S. S. (2018b). High temperature heat pumps: Market overview, state of the art, research status, refrigerants, and application potentials. *17th International Refrigeration and Air Conditioning Conference at Purdue, July 9-12, 2018*, 1–10. https://doi.org/10.1016/j.energy.2018.03.166

Arpagaus, C., Prinzing, M., Kuster, R., Bless, F., Uhlmann, M., Schiffmann, J., & Bertsch, S. S. (2019). High temperature heat pumps -Theoretical study on low GWP HFO and HCFO refrigerants. *ICR 2019, The 25th IIR International Congress of Refrigeration, August 24-30, Montréal, Québec, Canada*, 1–8. https://doi.org/10.18462/iir.icr.2019.259

BAFU. (2019). *Verordnung zur Reduktion von Risiken beim Umgang mit bestimmten besonders gefährlichen Stoffen, Zubereitungen und Gegenständen (Chemikalien-Risikoreduktions-Verordnung) (ChemRRV), Stand 9. Juli 2019: Vol. 814.81*. https://www.admin.ch/opc/de/classified-compilation/20021520/index.html

Eyerer, S., Dawo, F., Kaindl, J., Wieland, C., & Spliethoff, H. (2019). Experimental investigation of modern ORC working fluids R1224yd(Z) and R1233zd(E) as replacements for R245fa. *Applied Energy*, *240*(April), 946–963. https://doi.org/10.1016/j.apenergy.2019.02.086

Fleckl, T., Hartl, M., Helminger, F., Kontomaris, K., & Pfaffl. (2015). Performance testing of a lab-scale high temperature heat pump with HFO-1336mzz-Z as the working fluid. *European Heat Pump Summit 2015, October 20-21, Nuremberg, Germany*, 1–25.

Fukushima, M. (2018). Next Generation Low- GWP Refrigerants AMOLEA. *JRAIA Int. Symposium 2018*, 1–5.

Guo, Q., Chen, L., & Mizukado, J. (2019). Atmospheric degradation mechanism of Z/E-CF3CF=CHCl, CF3CF=CCl2, and CF2=CFCl initiated by OH radicals using a smog chamber with long-path FT-IR at 298 K. *Atmospheric Environment*, *218*(August), 116991. https://doi.org/10.1016/j.atmosenv.2019.116991

Hamacher, T. (2019). Höchsttemperaturwärmepumpe HeatBooster im industriellen Einsatz. *DKV-Tagung 2019, Ulm, 21.-23. Nov. 2019*, 1–9.

Helminger, F., Kontomaris, K., Pfaffl, J., Hartl, M., & Fleckl, T. (2016). Measured Performance of a High Temperature Heat Pump with HFO-1336mzz-Z as the Working Fluid. *ASHRAE 2016 Annual Conference, St. Louis, Missouri, 25-29 June 2016*, 1–8.

Henne, S., Shallcross, D. E., Reimann, S., Xiao, P., Boulos, S., Gerecke, A. C., & Brunner, D. (2012). Environmental impacts of HFO-1234yf and other HFOs. *ASHRAE/NIST Refrigerants Conference: Moving Towards Sustainability*, 182–194.

Honeywell. (2011). *Honeywell Genetron® Refrigerants, Brochure*. https://www.honeywell-refrigerants.com/europe/wp-content/uploads/2012/10/Honeywell-genetron-refrigerants-overview-brochure.pdf

Honeywell. (2013). *Solstice 1233zd(E) Technical Information* (pp. 1–8).

Innosuisse. (2019). *SCCER Efficiency of Industrial Processes (SCCER EIP)*. www.sccer-eip.ch

Kaida, T., Fukushima, M., & Iizuka, K. (2019). Application of R1224yd(Z) as R245fa alternative for high temperature heat pump. *ICR 2019, The 25th IIR International Congress of Refrigeration, August 24-30, Montréal, Québec, Canada*, 1–8.

Kobelco. (2019). *Water-cooled High Temperature Heat Pump "HEM-HR-GN/GL Series" using "Green Refrigerant" goes on sale*. https://www.kobelco.co.jp/releases/1201980_15541.html

Kontomaris, K. (2014a). HFO-1336mzz-Z: High Temperature Chemical Stability and Use as A Working Fluid in Organic Rankine Cycles, Paper 1525. *International Refrigeration and Air Conditioning Conference, Purdue, July 14-17, 2014*.

Kontomaris, K. (2014b). Zero-ODP, Low-GWP, Nonflammable Working Fluids for High Temperature Heat Pumps. *ASHRAE Annual Conference, Seattle, Washington, July 1, 2014*, 1–40.

Kujak, S., Schultz, K., & Sorenson, E. (2018). Experiences with next generation low GWP refrigerants in centrifugal chillers. *1st IIR International Conference on the Application of HFO Refrigerants, Birmingham, UK 2-5 September 2018*, 1–8. https://doi.org/10.18462/iir.hfo.2018.1110

Mateu-Royo, C., Navarro-Esbrí, J., Mota-Babiloni, A., Molés, F., & Amat-Albuixech, M. (2019). Experimental exergy and energy analysis of a novel high-temperature heat pump with scroll compressor for waste heat recovery. *Applied Energy*, *253*(June), 113504. https://doi.org/10.1016/j.apenergy.2019.113504

Myhre, G., Shindell, D., Bréon, F.-M., Collins, W., Fuglestvedt, J., Huang, J., Koch, D., Lamarque, J.-F., Lee, D., Mendoza, B., Nakajima, T., Robock, A., Stephens, G., Takemura, T., & Zhang, H. (2013). Anthropogenic and natural radiative forcing. In *Climate Change 2013: The Physical Science Basis. Contribution of Working Group I to the Fifth Assessment Report of the Intergovernmental Panel on Climate Change* (pp. 659–740). Cambridge University Press.

Nilsson, M., Risla, H. N., & Kontomaris, K. (2017). Measured performance of a novel high temperature heat pump with HFO-1336mzz-Z as the working fluid. *12th IEA Heat Pump Conference 2017, Rotterdam*, 1–10.

Patten, K. O., & Wuebbles, D. J. (2010). Atmospheric lifetimes and Ozone Depletion Potentials of trans-1-chloro-3,3,3-trifluoropropylene and trans-1,2-dichloroethylene in a three-dimensional model. *Atmospheric Chemistry and Physics*, *10*(22), 10867–10874. https://doi.org/10.5194/acp-10-10867-2010

Rached, W., Kim, S., & Abbas, L. (2018). Stable R-1233zd (E) for energy recovery applications. *1st IIR International Conference on the Application of HFO Refrigerants, Birmingham, UK, 2-5 September 2018*, 1–7. https://doi.org/10.18462/iir.hfo.2018.1137

Sulbaek Andersen, M. P., Schmidt, J. A., Volkova, A., & Wuebbles, D. J. (2018). A three-dimensional model of the atmospheric chemistry of E and Z-CF3CH=CHCl (HCFO-1233(zd) (E/Z)). *Atmospheric Environment*, *179*(44), 250–259. https://doi.org/10.1016/j.atmosenv.2018.02.018

Tokuhashi, K., Uchimaru, T., Takizawa, K., & Kondo, S. (2018). Rate Constants for the Reactions of OH Radical with the (E)/(Z) Isomers of CF3CF=CHCl and CHF2CF=CHCl. *The Journal of Physical Chemistry A*, *122*(12), 3120–3127. https://doi.org/10.1021/acs.jpca.7b11923

Viking Heat Engines. (2018). *HeatBooster HBS4: Industrial heat pump for clean energy production up to 160 °C*.

Wallington, T. J., Sulbaek Andersen, M. P., & Nielsen, O. J. (2015). Atmospheric chemistry of short-chain haloolefins: Photochemical ozone creation potentials (POCPs), global warming potentials (GWPs), and ozone depletion potentials (ODPs). *Chemosphere*, *129*, 135–141. https://doi.org/10.1016/j.chemosphere.2014.06.092

WMO (World Meteorological Organization). (2011). *Scietific Assessment of Ozone Depletion 2010, Global Ozone Research and Monitoring Project - Report No. 52, Geneva, Switzerland*.

ACKNOWLEDGEMENTS

This research project was part of the Swiss Competence Center for Energy Research – Efficiency of Industrial Processes (SCCER EIP, www.sccer-eip.ch) of the Swiss Innovation Agency Innosuisse. The authors thank Debra Carolina Cortés Gómez from the Institute for Microtechnology and Photonics (IMP) at the Eastern Switzerland University of Applied Sciences of Technology for the measurements of the acid numbers of the POE oils, and AGC Chemicals, Chemours, and ARKEMA for providing the refrigerant samples.